3-2-5 FMCW Ionosonde for the SEALION Project

NOZAKI Kenro

A portable low power FMCW ionosonde has been developed and deployed mainly at unmanned overseas observation points. Due to the low power of transmitting signals, there has been very little interference from existing radio systems around the FMCW ionosondes. The post-observation data processing offers wide possibilities in manipulating the observed data because the FMCW ionosonde records the entire baseband signal and measurement parameters are selected after observation. Output ionograms are equivalent to those of the routine ionosondes operated by the National Institute of Information and Communications Technology. FMCW ionospheric observation technology has been transferred to Kyushu University to aid mainly in studying the electric field by Doppler observation.

Keywords
FMCW, Ionosonde, DDS

1 Introduction

Ionosondes typically use a wide range of frequencies in the MF-HF band depending on the characteristics of the bottomside of the ionospheric region. Stationary ionosondes for routine observation at four domestic observatories and Antarctic Syowa Station have been successively developed by the National Institute of Information and Communications Technology (NICT)[1]-[3]. However, it is difficult to promptly initiate observation at a desired location with such a non-portable system. In addition, as each ionosonde is a pulse radar system with transmitting power of 10 kW, there requires accommodations between neighboring radio systems and making the system unsuitable for continuous observations.

As one of the pulse compression technology, FMCW (Frequency Modulated Continuous Wave) enables low transmitting power[4] and offers continuous observation without mutual interference with neighboring radio stations. Coupled with appropriately selected observation sequence and data processing, FMCW can provide exceptional flexibility in operation. The measurement technology of HF-band FMCW radar was first established in the 1970s. Barry[4] designed practical models by modifying a commercial synthesizer for faster frequency switching and later by adopting a micro-phase synthesizer in which the sweep voltage signal applied to a voltage-controlled oscillator (VCO) apart from synthesizer feedback loop.

FMCW exhibits its distinctive characteristic utility in bi-static observation in which the transmitting and receiving antennas are located sufficiently apart from each other. One of the highly adaptive applications is long-range oblique sounding. FMCW sounding signals from the icebreaker *Fuji* on the way to Antarctica and from Germany were monitored in Japan to examine propagation modes together with maximum usable frequency (MUF) and lowest usable frequency (LUF). Ichinose et al.[5] analyzed seasonal changes of magnetic disturbance effects on the propagation between Japan and Germany. Bi-static over-the-horizon FMCW radar has also been used to observe ocean waves by means of sky waves[6].

For mono-static observation which transmits radio waves vertically, Poole[7] and Poole and Evans[8] demonstrated that polarization mode separation, Doppler shift, and arrival angle observations could be established by means of an vertical incidence FMCW ionosonde with a peak power of 20 W. Oblique sounding was also conducted between the Antarctic SANAE Station and Grahamstown, South Africa. The FMCW ionosonde had thus been used in limited applications until sweep frequency generators and post-observation data processing became easily accessible.

In Japan, an ionosonde attached to the MU radar of Kyoto University was developed based on the FMCW technique[9]. Due to the limit of effective sweep range of the sweep synthesizer, observations were conducted by stepping up the sweep start frequency by 100 kHz. The FMCW ionosonde assembled by the Radio Research Laboratories (predecessor of NICT) for Antarctic observations[10] performed continuous observations at a fixed frequency as low as 20 W, and found wavy variations in the bottomside of the ionospheric region above Syowa Station[11]. Due to low capacity on the data processing, one observation was divided into about 100-kHz sweep units and it took about 15 minutes to obtain one ionogram.

With the onset of the 1990s, the direct digital synthesizer (DDS) operable in the HF band became increasingly popular, enabling an entire frequency band sweep with high precision. Advances in computer technology have also increased greater flexibility to the scope of observation control and data processing. Because of the strict regulation on transmitting radio wave qualities, it took a long time to negotiate before the Japanese Telecommunications Bureau agreed to issue the radio license, regardless of output power[12] and spurious intensity[13] that satisfied the Radio Act over the entire frequency range. For this reason, overseas observations took the lead. A portable ionosonde, developed for the West-Pac campaign near the geomagnetic equator in 1997[14] and observations in Fukui Prefecture in collaboration with the MU radar in 1998[15], employed domestically produced DDSs. The transmitter and receiver contained in trunk cases were transported as the hand baggage of one person. An ionosonde designed for the SEALION Project[16] in 2002 had its receiver/controller unit sizably digitized, featuring PLD (Programmable Logic Device) implementation in the second IF and subsequent circuits.

This paper provides preliminary insight into the principles of operation of the FMCW ionosonde in Section **2**, system construction in Section **3**, and some observational examples in Section **4**, mainly on the FMCW ionosonde developed for the SEALION Project.

2 Principles of operation

When the observation radio wave with frequency f varying linearly as $f = f_0 + \dot{f} \cdot t$ with time t is reflected by a moving target at range r and with line of sight velocity v as $r = r_0 + v \cdot t$, frequency difference f_b between the transmitting and receiving signals is expressed, under the condition of $v \ll c$, as

$$f_b(r,v) = \frac{2}{c}\left(r \cdot \dot{f} - v \cdot f_0\right) \qquad (1)$$

where $\dot{f}$ is the frequency sweep rate and c is the velocity of light. Frequency and time relation is shown in Fig. 1. The first term in the parenthesis on the right side of Equation (1) gives the frequency shift due to the range; the second term denotes the Doppler shift. In typical observations, $\dot{f}$ is set at around 100 kHz/s, and if the Doppler term is disregarded, the baseband frequency corresponding to 1000 km, the maximum height of the bottom of the ionospheric region would equal 667 Hz, thus enabling a narrower bandwidth of the IF stage than a pulse type ionosonde, and alleviating the effects of interference.

Poole[7] and Poole and Evans[8] operated an FMCW ionosonde using three-cell sound-

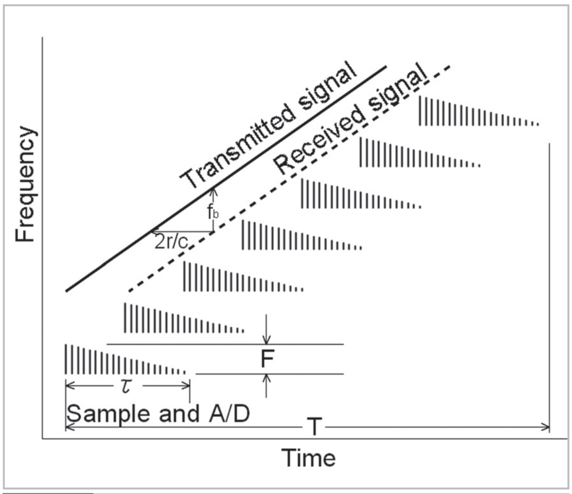

Fig. 1 FMCW radar system schematic

ing to confirm its applicability to polarization separation, Doppler observations, and arrival angle measurement. In contrast, our ionosonde is designed on the assumption that the Doppler velocity is obtained by converting the baseband signal twice[17][18].

2.1 Resolutions

The range resolution Δr and velocity resolution Δv are determined by the conditions of $f_b(\Delta f, 0)\cdot\tau = 1$ and $f_b(0, \Delta v)\cdot T = 1$, and can be expressed as follows:

$$\Delta r = \frac{c}{2\dot{f}\cdot\tau} = \frac{c}{2F} \tag{2}$$

$$\Delta v = \frac{c}{2f\cdot T} \tag{3}$$

As can be seen from Fig. 1, $F = \dot{f}\cdot\tau$ is a frequency width scanned at each sampling interval. On the basis of Eq. (2), Δr is determined solely by the frequency width used in the analysis, so that it can be established after the observation. Pulse radar requires a narrower pulse width for fine resolution, and then high transmitting peak power to achieve the required signal strength, but FMCW radar does not necessarily require the high transmitting power for fine resolution observation. Similarly to pulse radar, FMCW radar has its velocity resolution determined by Doppler observation time T.

2.2 Data processing gain

The FMCW is one of the spread spectrum methods. Frequency analysis on the baseband signal corresponds to the matched filter of spread spectrum communications. Signal amplitude is increased by the pulse compression ratio G after passage through the matched filter. G is defined as:

$$G = F\cdot\tau \tag{4}$$

where F and τ are the frequency scan width and the sampling duration, as shown in Fig. 1 respectively[19]. Assuming typical values of $\dot{f} = 100$ kHz/s and $\Delta r = 1$ km, Eq. (2) gives $\tau = 1.5$ sec and $F = 150$ kHz, then $G = 2.25\times10^5$ can be derived. Therefore, a FMCW radar system with a transmitting power of 10 W theoretically equals a pulse radar system of 2.3 MW peak power.

2.3 Transmit/receive switching

In mono-static FMCW observations, coupling between the transmitting and receiving antennas is inevitable in the MF-HF band used by ionosonde, such that a considerable part of emitted power from the transmitting antenna sneaks into the receiving antenna and suppresses the receiver. When a transmitting power of 40 dBm (10W) is fed to a conventional delta antenna, the typical ionospheric reflected signal strength is about −100 dBm at the receiver input. Because the coupling loss between the transmitting and receiving antennas placed perpendicularly is about 30 dB, direct waves sneaking into the receiving antenna from the transmitting antenna have strength of 10 dBm and by far exceed the receiver s dynamic range. As a solution to this problem, so-called Frequency Modulated Interrupted Continuous Wave (FMICW or Pulsed Chirp) is commonly used by alternating transmission and reception as shown in Fig. 2.

The signal reflected from the target at range r (and hence the delay $2r/c$) is effectively received upon arrival in the receiving window, but the signal arriving at the receiver

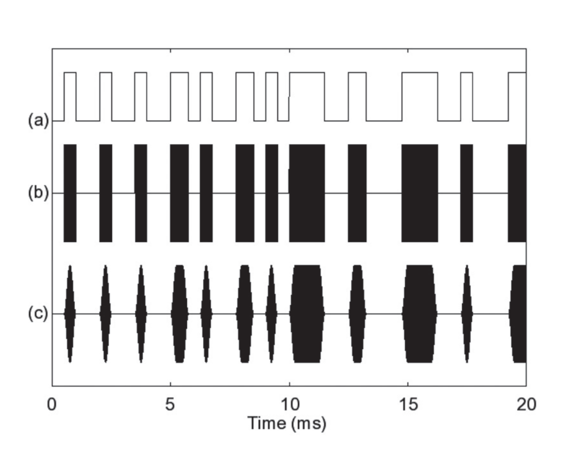

Fig.2 *Transmit/receive switching schematic*

(a) Transmit/receive switching signal.
(b) Transmitting signal interrupted according to (a).
(c) Transmitting signal with shaped envelop.

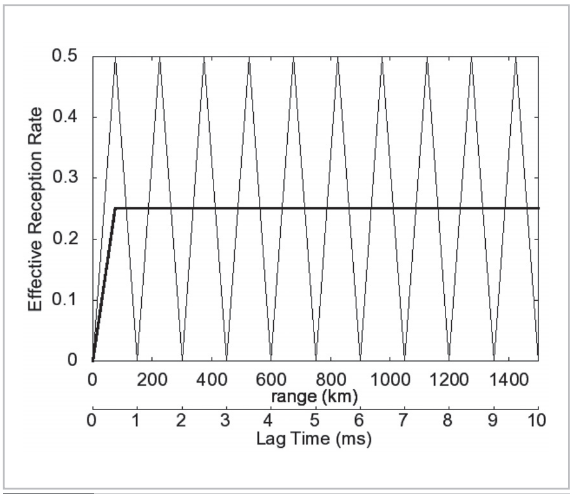

Fig.3 *Changes in receiving time ratio on transmit/receive switching*

The thin line denotes a repetition frequency having a symbol transmission interval of 0.5 ms, and the bold line designates transmit /receive switching with an M-sequence pseudorandom code by using a 10-stage shift register.

during transmission does not contribute to the observation. Assume transmit/receive switching signal $g(t)$ is as follows: $g(t)$=1 at transmission, and $g(t)$=0 at reception, then, the effective receiving time rate $\rho(r)$ of the echo from a target located at range r can be expressed as follows:

$$\rho(r)=\frac{\int g(t-2r/c)(1-g(t))\,dt}{\int dt} \qquad (5)$$

With transmit/receive switching in a fixed rectangular waveform, $\rho(r)$ would vary periodically between a maximum of 0.5 and a minimum of 0.0 with the range . A constant $\rho(r)$ independent on the range is obtained by random T/R alternation [20]. When using an M-sequence pseudorandom code having chip rate t_0 and n-stage shift register sequence length N=2^n-1, Equation (5) becomes

$$\rho(r)=\begin{cases}\dfrac{1}{4}\left(1+\dfrac{1}{N}\right)\dfrac{|2r/c-kNt_0|}{t_0} & (kN-1)\le\dfrac{2r}{c}\le kNt_0 \quad (k=0,1,2,,,)\\[2ex] \dfrac{N+1}{4N} & r:\text{otherwise above}\end{cases} \qquad (6)$$

Therefore, $\rho(r)$ would be 25% (constant) beyond range $r_0=ct_0/2$ for sufficiently large N.

Figure 3 shows the range variation of $\rho(r)$ for t_0 = 0.5 ms. The thin and bold lines indicate cases of transmit/receive switching in a fixed rectangular waveform (Fig. 2 a) and a pseudo-random code with n = 10 (Fig. 2 b), respectively. Poole [20] showed that $\rho(r)$ varies with range when the Q-sequence code signal, which is derived from the M-sequence code, is employed for alternating transmit/receive operations.

According to Iguchi [21], spectrum of interrupted frequency sweep signal $S(f)$ consists of monotonous carrier fc and the side-band due to switching as:

$$S(f) = \frac{N+1}{N}\pi^2A^2\left\{\delta(f-f_c) + \frac{1}{N}\left[\frac{\sin(\pi(f-f_c)t_0)}{\pi(f-f_c)t_0}\right]^2\sum_{\substack{k=-\infty\\k\neq0}}^{\infty}\delta\left(f-f_c-\frac{k}{T}\right)\right\} \qquad (7)$$

where, A denotes the amplitude of the carrier. The first term in the parentheses on the right side of Eq. (7) represents the carrier component, that is, the effective signal, and the second term represents a sideband due to alternating transmit/receive operations by the pseudo-random pulses. When the carrier is interrupted

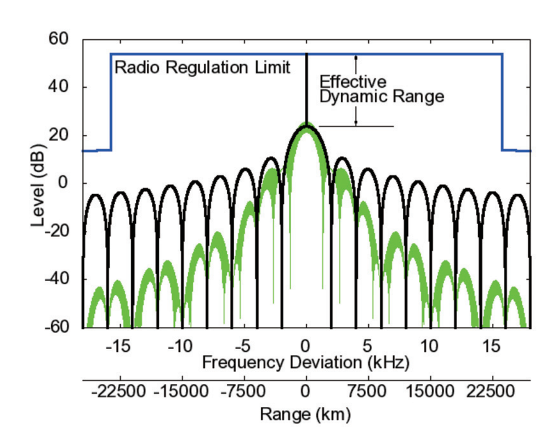

Fig.4 *Spectrum spread around the carrier by transmit/receive switching with pseudorandom code*

The black line denotes interruption of the carrier (Fig. 2 b), and the green line designates the result of amplitude modulation with a smooth envelope (Fig. 2 c). The blue line marks the limits to out-of-band radiation imposed by the Radio Regulatory Laws [13].

by an M-sequence pseudorandom code of n = 10 (Fig. 2 b), the sideband spreads widely from the level 30 dB below the carrier in the form of $(\sin f/f)^2$, thereby being considered a constant level over the observing range as indicated by a black line in Fig. 4. The signal reflected from the target also has a spread spectrum around the carrier given by Eq. (7), and all signals lower than 30 dB from the dominant echo are shielded. Even if the transmitting power is increased, the sideband level would be also lifted, leaving the apparent dynamic range unchanged at 30 dB. The spread echo spectrum disturbs the detection of scattered signals having significantly changing levels according to the range as with ocean wave radar, in contrast to harmless echoes that do not vary as much as reflections from the stratified ionospheric region. The ocean wave radar alternates transmission and reception by using monotonous signals in spite of range variation in $\rho(r)$ shown with the thin line in Fig. 3. Transmit/receive switching at a fixed frequency would turn the sideband into isolated peaks of switching frequency harmonics, thus allowing a weak received signal to be observed by flushing the switching frequency out of the IF band [21][22].

As the spread of spectrum by T/R switching is merely an obstruction to neighboring radio systems, excess spectrum is suppressed by smooth shaping of the switching signal as shown Fig. 2 (c) (see the green line in Fig. 4). The received signal is modulated with inverse of the T/R switching signal in the receiver. Iguchi [21] showed further increase in the sideband of the baseband signal.

3 System construction

As ionosondes are often installed in rural sites under inconvenient power and communication conditions, the system is designed to withstand self-sustained operation for a long period without maintenance. Remote control and data archiving are practicable, provided that network access is available. One entire observation system includes a main FMCW ionosonde and such peripherals as a pair of transmit/receive antennas, an antenna switch/attenuator, an RF wattmeter, coaxial arresters, a control PC, a network PC, and others. As an example, Figure 5 shows a block diagram of the system installed at Chumpon Campus, King Mongkut's Institute of Technology Ladkrabang (KMITL), the Kingdom of Thailand (CPN: 10.73ºN, 99.38ºE). Figure 6 shows photographs of the antenna and the system, respectively. Table 1 summarizes the key specifications. Observations normally take place at a frequency sweep rate of 100 kHz/s between 2 MHz and 30 MHz, and therefore, each session of observation takes 4 minutes and 40 seconds to complete.

A pair of crossed folded dipoles with terminators or delta loop antennas is stretched from the top of a 30-m tower. Since the observing frequency range is 10 times or more wide, traveling-wave antennas, though poor in efficiency, are used to achieve flat frequency characteristics in a simple setup.

The antenna selector SW/attenuator interconnects the transmitter/receiver and antennas only when the ionosonde is at work. The ionosonde is disconnected from the antenna

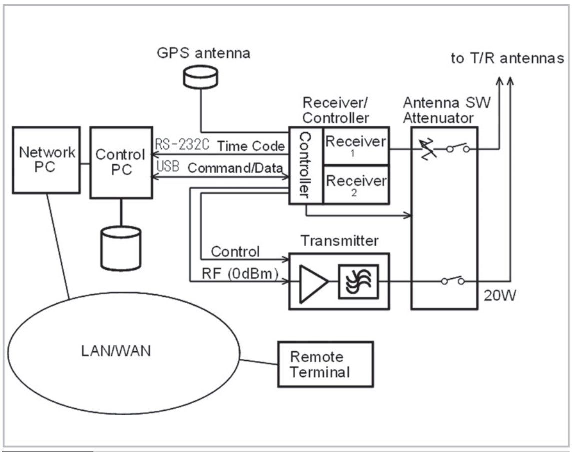

Fig.5 FMCW ionosonde system block diagram

Fig.6 FMCW ionosonde installed at Chumphon (CPN), Thailand

Upper: 30 m antenna tower.
Lower: (Right) from top to bottom: transmission-type wattmeter, transmitter, receiver, antenna selector switch/attenuator. (Left) quick-look ionogram displayed on the control PC.

Table 1 FMCW ionosonde key specifications

Observation mode	Linear FMCW/FMICW
Observation frequency	2 MHz ～ 30 MHz (programmable)
Frequency sweep rate	100/200/500 kHz/s
Transmit/receive switching signal	Square wave/M-sequence pseudorandom code
Chip rate	0.5 ms
Transmitting power	20 W (peak)
Receiver sensitivity	−132 dBm
Dynamic range	84 dB
Receiver bandwidth	500/1 k/2 kHz (synchronized with frequency sweep rate)
Interface to host PC	USB
Time signal to the host	RS-232C
Housekeeping data	Output/reflected power, controller/power amplifier temperature
Power supply	AC 50/60Hz 85～240V
Weight	40 kg or less

while stand by state to protect from lightning damage. The attenuator compensates for the difference in echo intensity between daytime and night.

As shown in Fig. 7, the receiver/controller houses two identical receivers as backups, allowing additional observational functions of direction-finding, polarization separation if an appropriate antenna is installed. The receiver first IF is 70.1 MHz and the second IF is 100 kHz. The second IF is digitally sampled at 1 MHz with 14 bits, followed by digital frequency conversion and bandwidth limiting on the PLD to generate a baseband signal. The second IF and subsequent stages are digitized to eliminate the bulky analog components and laborious adjustment tasks. As there is no tuning at the input stage of the receiver, all environmental radio waves of broadcasting and communications pile up above the echo signals at receiver input. Only MF broadcasting is eliminated by a 2 MHz high pass filter (HPF) at the front end of the receiver. A high intercept level module is selected for the Head Amplifier. Spiky pulses, generated when sweep frequency passes the strong interference carrier frequencies, are picked up by the noise blanker and eliminated by turning off the transmit/receive switch (T/R SW) placed downstream of the signal flow. During the transmitting sequence in mono-static ionosonde mode, the receiver input signal is cut off by turning off the gate switch and also the D/A converter of the DDS, so that the transmitting signal never leaks into the receiver. The switched signal is then envelope-shaped for suppressing ringing by the gain weighter, an analog multiplier subsequent to T/R SW.

Commands, baseband data, and housekeeping data are sent to and from the control PC via a USB interface. The control unit interprets a command and then settles DDS, T/R switching, and envelop shape, while processing the received baseband signal. As the control PC sets parameters and issues an observa-

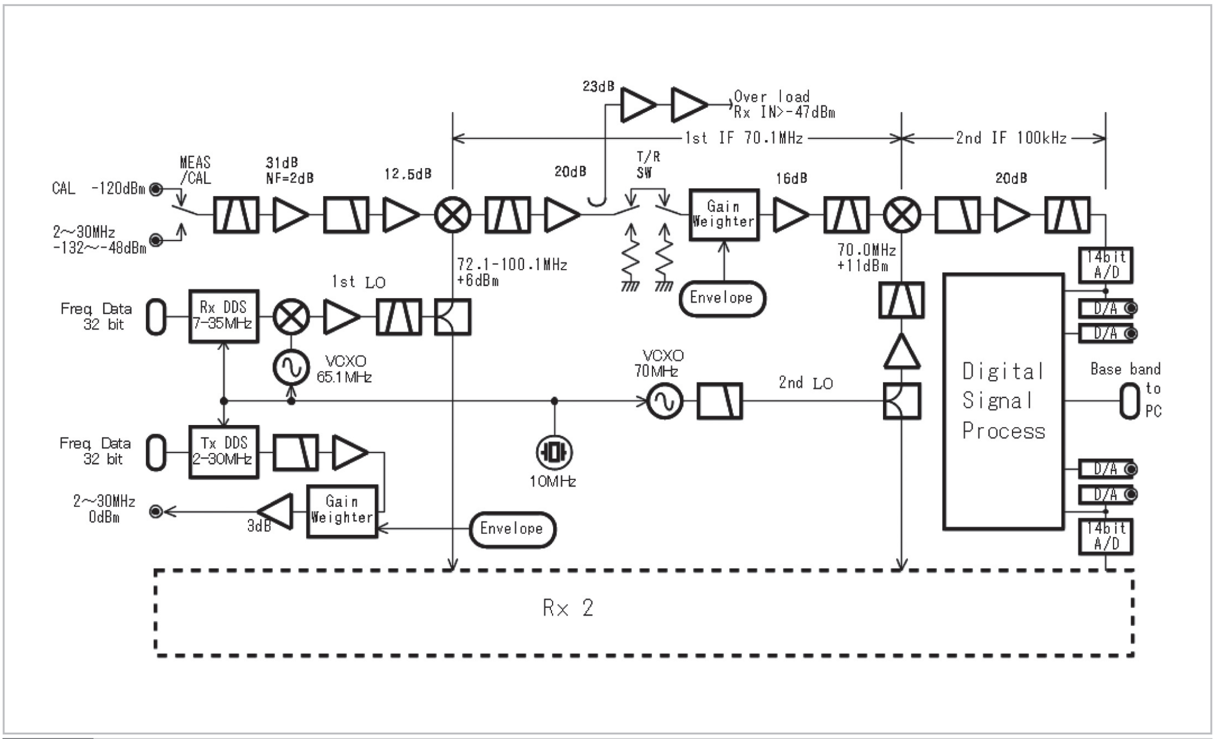

Fig.7 Receiver/Controller block diagram

tion start signal for each session of observation, the controller starts observation in sync with 1-second pulses from the GPS clock, and the baseband signal is transferred from the controller to the control PC. The GPS clock sends time codes to the control PC via an RS-232C interface every second. Observation can be triggered by any delay time from the 1-second pulse in order of microseconds so that interference between neighboring stations can be avoided by adjusting each offset time.

All signals within the receiver/controller are generated in sync with the signal from the built-in, 10-MHz high-stability crystal oscillator. Phase continuous sweep frequency signals, the fundamental elements of FMCW radar, are generated in 1 Hz steps using DDSs individually for transmission and reception. The transmit and receive frequencies can be staggered to generate pseudo-echoes at testing. The DDS clock frequency is 80 MHz; the transmitting frequency is generated directly between 2 and 30 MHz. For the first receiver local frequency, DDS output frequency is doubled and then converted with a fixed frequency to 72.1 ~ 100.1 MHz. The DDS is 32 bits wide for frequency and 12 bits wide for amplitude. Spurious level of the D bit D/A conversion is not more than

$$Spur \approx -20\log\left(2^{D}\right) \qquad [\text{dBc}] \qquad (8)$$

according to Reference [20]. Therefore, the spurious strength attributable to the DDS is held to -70 dBc or below.

As shown in Fig. 2, the swept-frequency signal generated in the transmit DDS is interrupted by a pseudorandom signal and envelope shaped before being directed to the transmitter. The transmitter amplifies the input signal of 0 dBm and sends it through the Low Pass Filter (LPF) block to the transmitting antenna with 20 W peak level. Because of the wide frequency range, a tune-less type amplifier is employed. A C-MOS FET Class A-B push-pull module is employed for the final stage, expecting low spurious level although low efficiency. A simple transmitting antenna is assumed as mentioned above, and the amplifier works under a mismatched condition. However, the amplifier is further protected by a relay at the extremely degraded VSWR. The LPF block consists of low pass filters varying in cutoff frequency by $\sqrt{2}$ times from each other in order to suppress harmonics. As the observed frequency is increased, an appropriate filter is selected from the controller.

The control PC issues commands to the control unit according to the observation schedule. After an observation sequence, a brief ionogram is drawn for a quick look and the data compressed file of the baseband signal is stored in a storage device. Although entire baseband signal consumes a large size of strage, it provides greater freedom in the work of generating ionograms, h'-t plots and more for analysis. As the control PC focuses on the tasks of controlling the ionosonde and receiving data, the network PC takes charge of transmitting data to and from the outside of the site, updating the observation schedule, providing the Internet firewall protection, and other tasks.

4 Observations

4.1 Ionosonde observations

The FMCW ionosonde affords greater freedom in post-processing by recording the entire baseband signal. Ionograms equivalent to the domestic routine observations are generated and then the ionospheric parameters are extracted by commonly utilizing the scaling system for the stationary ionosondes (http://wdc.nict.go.jp/IONO/index.html). Frequency scan F used to draw a frequency line is determined as $F = c/2\Delta r$ from Eq. (2) for given range resolution Δr. Frequency step in an ionogram is discretionally selected by duplicating a data sample as shown in Fig. 1.

Figure 8 shows the spread F phenomenon observed at CPN on July 8, 2003. Ionograms drawn every 20 minutes for 3 MHz ～ 9 MHz are put in order. The time is given by UT. Sunset time on that day was 11:49UT. It is clear that F-region echo rose up due to E×B drift after sunset and developed into the spread F near the apex. Vertical streaks in each ionogram indicate intense interferences. Sufficient echo strength is obtained under the stratification conditions before and after spread F.

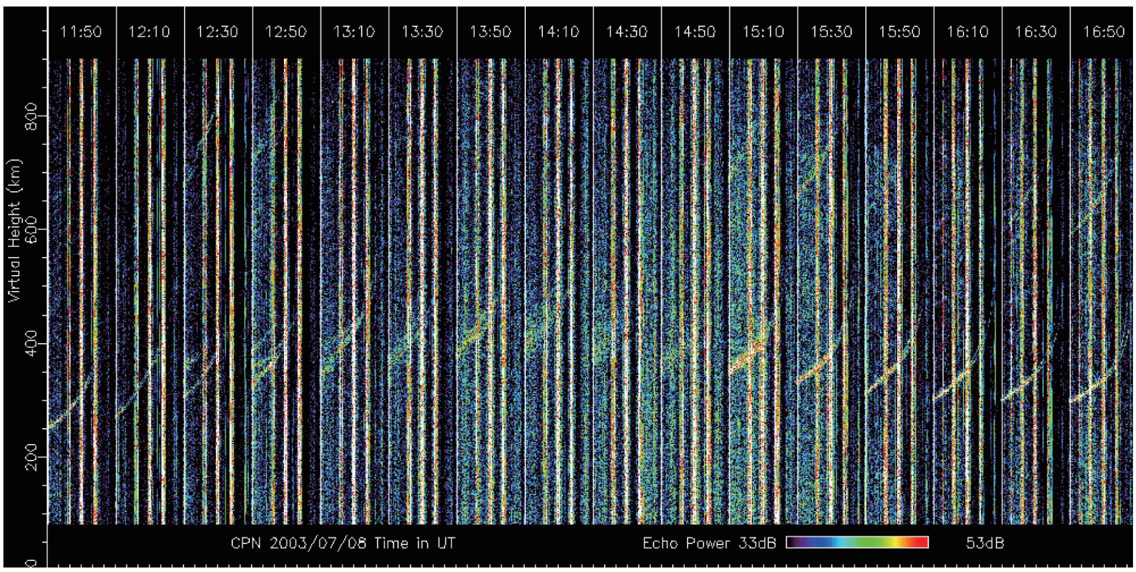

Fig.8 Spread F sequence above CPN

Under the spread *F* condition, however, the small cross section of each ionized patch requires higher transmitting power or more detailed threshold processing in drawing an ionogram.

4.2 h'-t observations

Collaborative observation with MU radar at Shigaraki, Shiga Prefecture (34.9°N, 136.1°E) was conducted during the summers from 1998 to 2002 when sporadic E (*Es*) was active. The FMCW ionosonde was installed at Sabae, Fukui Prefecture (36.0°N, 136.3°E) just below the E region field aligned irregularity (FAI) illuminated by the MU radar [15]. Because the FAI has a structure along geomagnetic field line B_0 as shown in the schematic diagram of location in Fig. 9, the cross section of FAI scattering has a maximum value in the plane perpendicular to the geomagnetic field line. The radio waves transmitted northward from MU radar are strongly scattered by the E-region FAI just above Sabae. The MU radar has a beam width of 4.5°. Although the FMCW ionosonde has a beam width of about 60°, it only observes echo signals reflected from the surface perpendicular to the line of sight.

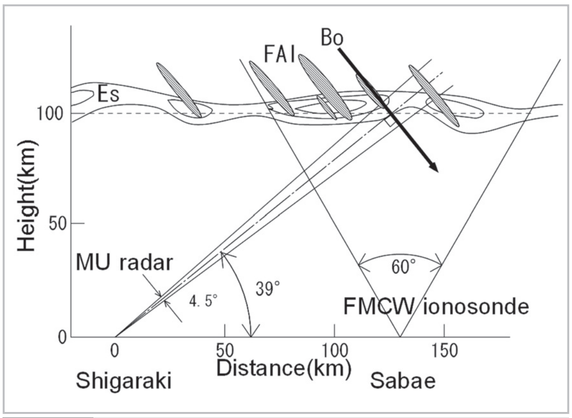

Fig.9 *Antenna configuration of MU radar and FMCW ionosonde in collaborative observations* [15]

At Sabae site, an aluminum pole about 15 m high was erected on top of an elevator tower on a five-story building, and folded dipole antennas with terminators were stretched on the rooftop as ionosonde transmitting and receiving antennas. The antennas were removed prior to snowfall in winter. To study the details of Es, the ionosonde was swept through a narrow frequency range minute-by-minute, and altitude changes with certain fixed frequencies were plotted with a resolution of 1.5 km. Simultaneous observations of the ionosonde h'-f and MU radar FAI scattering are shown in Fig. 10 [15]. Quasi periodic (QP) echoes were observed as follows: 2000/06/01 19:45∼20:25 LT, 20:40∼21:30 LT, and 06/02 00:10∼02:10 LT. The Es above Sabae, descended slowly from 120 km to 100 km during the period. The echo altitude observed by the ionosonde coincided with the strongest QP echo scattering altitude observed by the MU radar. Echo altitude variations at 4, 5 and 6 MHz well corresponded to the generation of QP echoes, but not with 3 MHz, thereby suggesting that the generation of QP echoes requires a certain electron density.

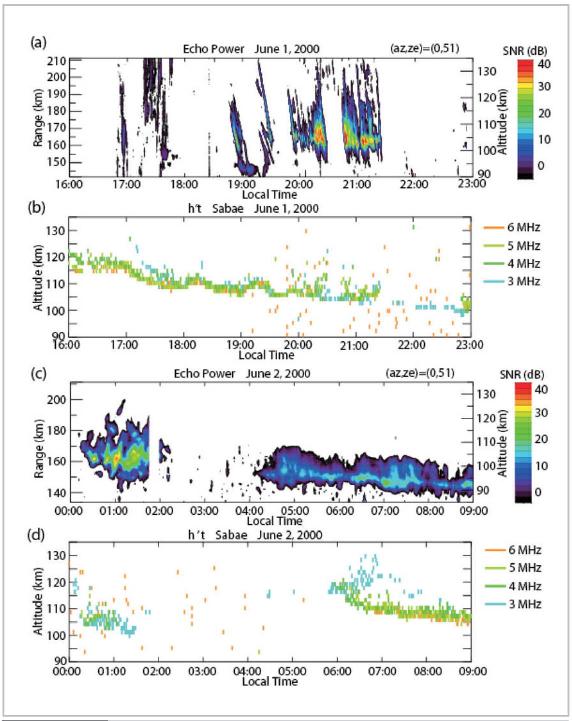

Fig.10 *Changes in altitude of Es by MU radar (a), (c) and multiple frequency h′-t plots (b), (d)* [15]

4.3 Doppler observation

When the eastward electric field appears in the ionospheric region, charged particles move perpendicular to the geomagnetic field

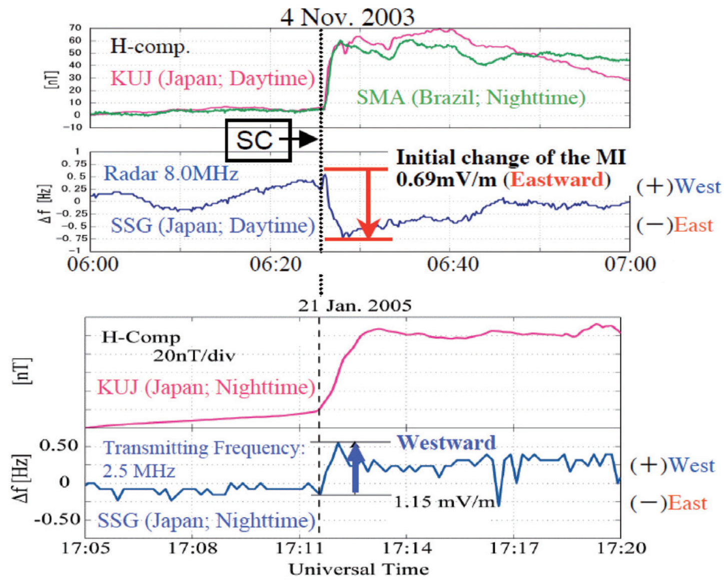

Fig.11 *Electric field observations in FMCW radar Doppler mode at geomagnetic SC* [24]

Upper case: SSG in daytime.
Lower case: SSG in nighttime.

due to E×B drift. Doppler observations make it possible to measure the electric field through the drift velocity. The ionosondes simultaneously observe the range and velocity, while HF standard-wave Doppler observation only provides velocity information. Figure 11 shows Doppler variations at the geomagnetic SC event observed at Sasaguri (SSG: 32.56ºN, 129.24ºE), Fukuoka Prefecture [24]. The upper case is SC phenomena at SSG in the daytime, indicating an eastward electric field. At SC, the magnetosphere is compressed, resulting in an increased geomagnetic field strength at both Kuju (KUJ: 32.71ºN, 133.19ºE) near SSG and at Santa Maria, Brazil (SMA: 29.97ºS, 57.86ºW), on the opposite side of the earth. The lower case shows SC phenomena at SSG in the nighttime, indicating that the electric field is impressed in the direction opposite to that in the daytime.

5 Concluding remarks

Because FMCW observations transmit the signal energy spread into time and frequency, a low-power advantage is exhibited on fine range resolution and a long interval observation. Because transmit/receive alternation is indispensable to HF mono-static observation, vertical incidence ionosonde cannot be totally utilized the FMCW pulse compression advantage. Yet, the FMCW ionosonde permits low-power observation and retains great usefulness as a compact portable observation apparatus. Low transmitting power results in no claims from nearby radio systems in Japan and in East Asia. Results of the mobile observations were utilized to decide the permanent observation point in the SEALION Project [16]. The ionosonde is designed to satisfy the requirements for transmitting power and unwanted spurious radiation stipulated in Japan's Radio Act over the observing frequency range, thereby making observation possible when and where required.

The FMCW ionosonde has also been used at Kyushu University, which conducted Doppler observations at Sasaguri, Fukuoka Prefecture, as well as in Russia and the Philippines, for correlative observations with various geomagnetic and ionospheric phenomena such as propagation of the DP2 field to low latitude and geomagnetic pulsations along with SC events[24][25].

Appreciating the FMCW advantages of low power, low EMC, and high reliability, a stationary FMCW ionosonde is being developed for the next generation of Antarctic observation apparatus. Interference will be highly eliminated by a front end band-pass filter varying in sync with the frequency sweep. The observation frequency range is planned to reduce the lower limit to 0.5 MHz and upper limit to 16 MHz according to the ionospheric characteristics above the Antarctica.

References

1 T. Koseki, T. Takeuchi, K. Ishizawa, S. Ito, and Y. Kuratani, “The 9-B type ionosonde of the Radio Research Laboratories,” Rev. RRL., Vol. 26, No. 139, pp. 679–691, 1980.

2 Radio Research Laboratories of Ministry of Posts and Telecommunications Ed., “Progress of ionosondes in Japan,” 1984. (in Japanese)

3 H. Kato, “5-1 Ionospheric observation and observation information processing system,” Rev. CRL, Vol. 48, No. 4, pp. 121–127, 2002.

4 G.H. Barry, “A low-power vertical-incidence ionosonde,” IEEE Geosci. Electron., Vol. GE-9, No. 2, pp. 86–89, 1971.

5 M. Ichinose, S. Fujii, and K. Nozaki, “Geomagnetic disturbance effects on usable frequency bands for a long-distance HF path,” Jour. RRL, Vol. 30, No. 130/131, pp. 143–150, 1983.

6 M. Kotaki, “Skywave radar,” Rev. RRL, vol. 29, No. 151, pp. 447–465, 1983.

7 A.W.V. Poole, “Advanced sounding 1. The FMCW alternative,” Radio Sci., Vol. 20, No. 6, pp. 1609–1616, 1985.

8 A.W.V. Poole and G.P. Evans, “Advanced sounding 2. First results from an advanced chirp ionosonde,” Radio Sci., Vol. 20, No. 6, pp. 1617–1624, 1985.

9 T. Sato, S. Fukao, T. Tsuda, and S. Kato, “Low power digital ionosonde,” Proc. FY86 RASC and 1st MU radar joint symposium, pp. 59–65, 1986. (in Japanese)

10 K. Nozaki and T. Kikuchi, “A new multimode FM/CW ionosonde,” Mem. Ntnl. Inst. Polar Res. Spec. Issue, No. 47, pp. 217–224, 1987.

11 K. Nozaki and T. Kikuchi, “Preliminary results of the multimode FM/CW ionosonde experiment,” Proc. NIPR Symp. Upper Atmos. Phys., No. 1, pp. 204–209, 1988.

12 Article 14, Ordinance Regulating Radio Equipment.

13 Table 3, Ordinance Regulating Radio Equipment.

14 T. Maruyama, K. Nozaki, M. Yamamoto, and S. Fukao, “Ionospheric height changes at two closely separated equatorial stations and implications in spread F onsets,” JATP, Vol. 64, pp. 1557–1563, 2002.

15 T. Ogawa, O. Takahashi, Y. Otsuka, K. Nozaki, M. Yamamoto, and K. Kita, “Simultaneous middle and upper atmosphere radar and ionospheric sounder observations of midlatitude E region irregularities and sporadic E layer,” JGR., Vol. 107, No. A10, p. 1275, 2002.

16 T. Maruyama, S. Saito, M. Kawamura, K. Nozaki, J. Uemoto, T. Tsugawa, H. Jin, M. Ishii, and M. Kubota, “Outline of the SEALION Project and Initial Results,” Special issue of this NICT Journal, 3-2-1, 2009.

17 T. Umehara, Y. Ohno, and T. Iguchi, “HF ocean radar 5. Signal processing for the HF ocean radar,” Rev. CRL, Vol. 37, No. 3, pp. 383–391, 1991.

18 D.E. Barrick, “FM/CW radar signals and digital processing,” NOAA Tech. Rep. ERL 283-WPL 26, 1973.

19 M. Skolnik, “Introduction to radar systems 2nd Edition,” McGraw-Hill, 1971.

20 A.W.V. Poole, “On the use of pseudorandom codes for chirp radar,” IEEE Trans. Antennas Prop., Vol. AP-27, No. 4, pp. 480–485, 1979.

21 T. Iguchi, “HF ocean radar 3. On the transmit/receive switching wave form for FMICW HF ocean radar,” Rev. CRL, Vol. 37, No. 3, pp. 361–374, 1991.

22 K. Nozaki, “HF ocean radar 4. Configuration of the HF ocean radar system,” Rev. CRL, Vol. 37, No. 3, pp. 375–382, 1991.

23 “Motorola 120DDSEVK Direct Digital Synthesizer Users Manual,” Motorola Inc., 1992.

24 K. Yumoto, A. Ikeda, M. Shinohara, T. Uozumi, K. Nozaki, S. Watari, K. Kitamura, V.V. Bychkov, and M. Shevtsov, “Electric and magnetic field variations at low and equatorial latitudes during SC, DP2, and Pi2 events,” Adv. In Geosciences, Vol. 14 (Solar Terrestrial), 2009, printing.

25 A. Ikeda, K. Yumoto, M. Shinohara, K. Nozaki, A. Yoshikawa, M.G. Cardinal, B.M. Shevtsov, V.V. Bychkov, Q.M. Sugon Jr, and D. McNamara, “Ionospheric observation using FM-CW radar array,” Adv. In Geosciences, 2011, printing.

NOZAKI Kenro
Telecom Engineering Center
Space Environment